# Identification of Lipid-Accessible Sites on the *Nephrops* 16-kDa Proteolipid Incorporated into a Hybrid Vacuolar $H^+$-ATPase: Site-Directed Labeling with *N*-(1-Pyrenyl)cyclohexylcarbodiimide and Fluorescence Quenching Analysis†

Michael Harrison,*,‡ Ben Powell,‡ Malcolm E. Finbow,§ and John B. C. Findlay‡

*School of Biochemistry and Molecular Biology, University of Leeds, Leeds, U.K., and CRC Beatson Laboratories, Beatson Institute for Cancer Research, Glasgow, U.K.*

*Received January 24, 2000; Revised Manuscript Received March 22, 2000*

ABSTRACT: Proton translocation by the vacuolar $H^+$-ATPase is mediated by a multicopy transmembrane protein, the 16-kDa proteolipid. It is proposed to assemble in the membrane as a hexameric complex, with each polypeptide comprising four transmembrane helices. The fourth helix of the proteolipid contains an intramembrane acidic residue (Glu140) which is essential for proton translocation and is reactive toward *N*,*N*′-dicyclohexylcarbodiimide (DCCD). Current theoretical models of proton translocation by the vacuolar ATPase require that Glu140 should be protonated and in contact with the membrane lipid. In this study we present direct support for this hypothesis. Modification with the fluorescent DCCD analogue *N*-(1-pyrenyl)cyclohexylcarbodiimide, coupled to fluorescence quenching studies and bilayer depth measurements using the parallax method, was used to probe the position of Glu140 with respect to the bilayer. Glutamate residues were also introduced mutagenically as targets for the fluorescent probe in order to map additional lipid-accessible sites on the 16-kDa proteolipid. These data are consistent with a structural model of the 16-kDa proteolipid oligomer in which the key functional residue Glu140 and discrete faces of the second and third transmembrane helices of the 16-kDa proteolipid are exposed at the lipid−protein interface.

The vacuolar $H^+$-ATPases are a class of ATP-driven proton pumps, playing a pivotal role in eukaryotic cell physiology. Located within the endomembrane system, or at the plasma membrane of some cell types, they generate the protonmotive force required to drive secondary transport processes or to generate acidic conditions which are essential for the function of many intracellular compartments (*1*, *2*). The overall architecture of the vacuolar $H^+$-ATPases (V-ATPases)[1] resembles that of the $F_1F_0$-ATPase, each comprising a soluble catalytic domain ($F_1$ or $V_1$) connected to a membrane-bound proton-translocating domain ($F_0$ or $V_0$) via one or more "stalk" structures (*3*, *4*). In the case of the $F_1F_0$-ATPase, it has been clearly demonstrated that changes in ATP/ADP binding induce rotation of a structural complex comprising a central stalk fixed to membrane subunits of $F_0$ (*5*, *6*). However, the precise mechanism that translates this rotation into proton movement remains uncertain. Similarities in the macromolecular appearance of the V- and F-type ATPases, and between sequences of some $V_1$ and $F_1$ subunits (*1*), suggest that the two enzymes may operate via similar rotational mechanisms, but this remains to be experimentally demonstrated.

A family of very hydrophobic membrane proteins, the proteolipids, are intimately involved in proton translocation through both the $V_0$ and $F_0$ sectors. In the V-ATPase this is the highly conserved 16-kDa proteolipid, whereas in the F-ATPase it is the 8-kDa subunit c. Both proteolipids are soluble in organic solvents and contain a DCCD-reactive acidic residue located within a transmembrane region which is essential for proton translocation (*7*, *8*). In the case of the 16-kDa proteolipid, this key residue is Glu140. The two proteolipid species also share limited sequence similarity, suggesting that they may have arisen from a common progenitor gene, with the 16-kDa proteolipid constituting a tandem repeat of its smaller relative (*9*). The high degree of conservation between 16-kDa proteolipids means that, in some cases, foreign proteolipids may functionally substitute for related proteins in heterologous expression studies. The 16-kDa proteolipid from the arthropod *Nephrops norvegicus* has been studied extensively in our laboratory and substitutes for the proteolipid product of the *VMA3* gene in *Saccharomyces cerevisiae* (*10*). In its native tissue, this protein forms structures which are reminiscent of gap junctions and which are devoid of other V-ATPase subunits or other proteolipid species. In addition to the heterologously expressed proteolipid representing a convenient vehicle for mutagenesis studies, these proteolipid-enriched membranes are also amenable to electron microscopy (*11*), AFM (*12*), and spectroscopic analyses (*13*). Data from a number of comple-

†This work was supported by The Wellcome Trust in the form of a career development fellowship to M.H. (Grant 042226/Z/94) and equipment grants to the Leeds Biomolecular Analysis facility.

* Corresponding author. E-mail: M.A.Harrison@leeds.ac.uk. Tel: (+44) (0)113 2333152. Fax: (+44) (0)113 2333167

‡ University of Leeds.

§ Beatson Institute for Cancer Research.

[1] Abbreviations: V-ATPase, vacuolar $H^+$-ATPase; DCCD, *N*,*N*′-dicyclohexylcarbodiimide; DOXYL, 4,4-dimethyloxazolidine-*N*-oxyl; PCD, *N*-(1-pyrenyl)cyclohexylcarbodiimide; NEM, *N*-ethylmaleimide; nSLPC, 1-palmitoyl-2-(*n*-DOXYL)stearoyl-*sn*-glycero-3-phosphocholine spin-labeled at position *n*; TEMPO, 2,2,6,6-tetramethyl-1-piperidine-*N*-oxyl.

10.1021/bi000159o CCC: $19.00 
Published on Web 05/31/2000

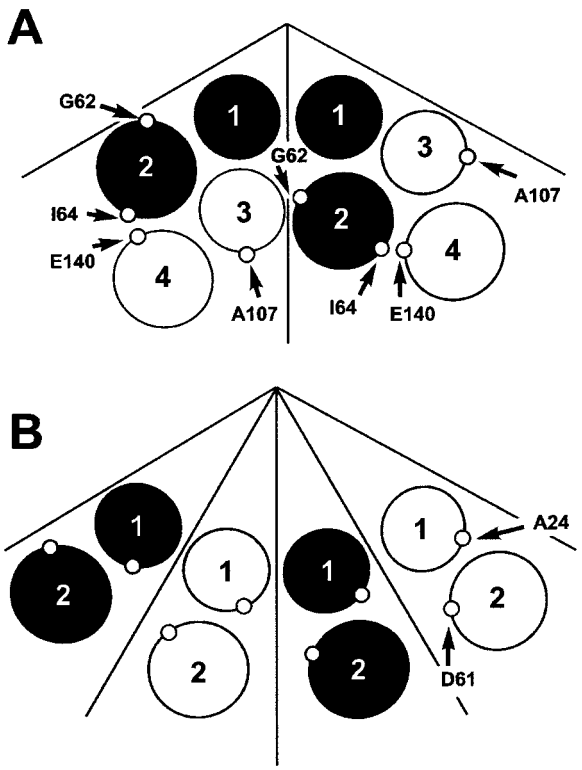


FIGURE 1: Models of helical packing and membrane organization for the 16-kDa and subunit c proteolipid oligomers. Transmembrane helices of the 16-kDa (A) and subunit c (B) proteolipids are represented as circles, viewed from the cytoplasmic surface. Helices of the 16-kDa proteolipid are arranged according to published disulfide cross-linking and cysteine labeling data (*18*, *19*). Paired helices are shaded to illustrate the tandem repeat relationship with subunit c. Gly62 and Glu140 of the 16-kDa species correspond to Asp61 of subunit c, in the first and second halves of the tandem repeat structure, respectively. Ala24 of subunit c corresponds to Ala107 of the V-ATPase proteolipid (see Figure 3). The helical organization in (A) predicts lipid exposure of Glu140 and the faces of helices 2 and 3 which contain Ile64 and Ala107, respectively.

mentary experimental approaches applied to different forms of the same protein can therefore be converged to produce an overall structural appreciation of the proteolipid assembly.

Determination of the structure of the subunit c monomer by NMR (*14*, *15*), coupled to cysteine cross-linking studies (*16*), has led to the proposal of structural models for the proteolipid dodecamer in $F_0$ (*15*, *17*). These in turn provide a solid framework on which to build plausible functional models of proton translocation through $F_0$. A more speculative structural model for the V-ATPase proteolipid oligomer has been proposed on the basis of cysteine cross-linking and labeling data (*18*, *19*). This model (outlined in Figure 1), which is consistent with available biophysical data, shows parallels with current experimentally derived models of subunit c organization in $F_0$ (*15*−*17*). According to the model, the 16-kDa proteolipid assembles as a hexamer of four-helical bundles, with helix 1 lining a central pore and helix 4 at the periphery of the complex. Helices 2 and 3 form the principal intermolecular contacts within the oligomer. The model predicts not only that the functionally critical Glu140 will be lipid-exposed but also that sites on helices 2 and 3 must be oriented toward the lipid phase (Figure 1). To test these predictions, and to provide independent experimental support for this model, we have used a site-specific labeling strategy in which the key Glu140 of the 16-kDa proteolipid is modified by reaction with a lipid-soluble fluorescent analogue of DCCD, an approach previously used with the $F_1F_0$-ATPase (*20*). Measurement of fluorescence yield in the presence of membrane-soluble quenchers is used to determine exposure of the bound fluorophore to the lipid phase and to estimate its depth in the bilayer. We have further exploited the specificity of the lipophilic carbodiimides to assay the accessibility of glutamate residues introduced mutagenically into the 16-kDa proteolipid. The relative reactivity of each introduced residue to the fluorescent carbodiimide provides information regarding the proximity of key sites on the proteolipid to the lipid phase, supporting a model of proteolipid organization within the membrane.

## EXPERIMENTAL PROCEDURES

*Plasmid Construction and Mutagenesis*. Isolation of the cDNA for the *Nephrops* 16-kDa proteolipid and construction of the hexahistidine-tagged derivative have previously been detailed (*10*, *11*). Mutagenesis of the 16-kDa proteolipid was performed by a PCR-based method (*21*), using as template a cDNA in which the wild-type Glu140 had been mutated to glycine. Mutations were confirmed by automated sequencing using the ABI Prism system. For constitutive expression in *S. cerevisiae* (strain W303-1B; *MAT*α, *his3*, *ade2*, *trp1*, *ura3*, *vma3*::*LEU2*), proteolipid cDNAs were subcloned into the 2$\mu$-based vector pPMA1 (*18*). Cells were transformed with pPMA1 vectors by the lithium acetate procedure (*22*). Transformants were routinely grown on minimal media (0.67% w/v yeast nitrogen base, 1% glucose) buffered to pH 5.5 with 25 mM MOPS/MES and supplemented with the appropriate amino acids for maintaining selection. To test for complementation of the *vma3* mutation, transformants were plated onto yeast extract−peptone−dextrose plates buffered to pH 7.5 (*18*).

*Protein Labeling and Purification.* Isolation of proteolipid-enriched membranes from *Nephrops* has been described previously (*11*). Vacuolar membranes were isolated from *Saccharomyces* using the method of Uchida et al. (*23*). Glycerol gradient fractionation of solubilized vacuolar membranes and purification of $V_0$ membrane sectors by $Ni^{2+}$-NTA affinity chromatography were performed as described (*10*). ATPase activities were determined as release of inorganic phosphate from MgATP as detailed in ref *18*. Purified vacuolar or native *Nephrops* membranes (0.5 mg of protein/mL) in 10 mM Tris-HCl, 0.1 mM EDTA, and 10% (v/v) glycerol were labeled with PCD (20 $\mu$M) for 3 h at 30 °C, then recovered, and washed twice by centrifugation at 100000*g* in a Beckman TLA100.2 rotor. Extraction of fluorescently labeled proteolipids with chloroform/methanol, SDS−PAGE, immunoblotting, and protein assays were performed as described in ref *19*.

*Reconstitution of $V_0$ Sectors.* Affinity-purified $V_0$ sectors were reconstituted into liposomes according to the method described in ref *24*, at a lipid:protein ratio of 100:1. Most efficient reconstitution was found with liposomes containing phosphatidylcholine, phosphatidylethanolamine, phosphatidylinositol, and phosphatidylserine in a molar ratio of 5:1:1:1. For fluorescence quenching experiments, 1-palmitoyl-2-(*n*-DOXYL)stearoyl-*sn*-glycero-3-phosphocholine, spin-

labeled at either the C5 (5-SLPC) or C12 (12-SLPC) position in the stearoyl chain, was substituted for unlabeled phosphatidylcholine to give varying mole ratios of spin-label lipid/total lipid. Proteoliposomes were formed in 10 mM HEPES−NaOH, pH 7.9, and stored at −70 °C in the same buffer. Lipids were purchased from Avanti Polar Lipids, Alabaster, AL.

*Fluorometry*. Fluorometric measurements were made with 10 $\mu$g of total membrane protein in a cuvette volume of 2 mL. Fluorescence emission in the range 355−455 nm was measured at 25 °C, with excitation at 342 nm, using a Perkin-Elmer LS50 scanning spectrofluorometer. Excitation and emission monochromator slit widths were set at 10 nm. For titrations of fluorescence yield with varying concentration of quencher, the quenching species was added to membranes from stock solution, with equilibration for 5 min prior to recording spectra. The depth of the fluorophore in the membrane was calculated by the parallax method (*25*), using PCD-labeled $V_0$ sectors reconstituted into liposomes containing varying mole ratios of spin-labeled phosphatidylcholine. Calculations were made according to the equation:

$$Z_{cF} = L_{c1} + \{[(-1/\pi C)\ln(F_1/F_2) - L_{21}^2]/2L_{21}\}$$

where $Z_{cF}$ is the distance of the fluorophore from the bilayer center, $L_{cl}$ is the distance between a shallow quencher (quencher 1) and bilayer center, and $L_{21}$ is the difference in depth between a shallow quencher 1 and a deep quencher 2. $C$ is the two-dimensional quencher concentration in the plane of the bilayer, calculated as the mole fraction of spin-labeled quencher lipid in total lipid divided by the surface area of a lipid molecule [assumed to be 70 Å$^2$ (*25*)]. Distances from shallow quencher 1 (5-SLPC) and deep quencher 2 (12-SLPC) to the bilayer center are assumed to be 12.15 and 5.85 Å, respectively (*25*, *26*). $F_1$ and $F_2$ are the relative fluorescence yields in the presence of quenchers 1 and 2, respectively.

*Mass Spectrometry.* Native *Nephrops* membranes containing PCD-modified proteolipid were solubilized with chloroform/methanol/formic acid/water (2:1:1:0.1), and insoluble material was removed by centrifugation. Solubilized protein was separated from lipid and free PCD by size exclusion chromatography with Sephadex LH20 resin (Pharmacia) using the same solvent. Concentrated fractions containing the proteolipid were analyzed by electrospray mass spectrometry using a Platform II (Micromass, Altrincham, U.K.) single quadrupole instrument. Positive ionization electrospray was used for the analysis using a capillary voltage of 3.5 kV and a counter electrode of 0.5 kV. Data were collected over the appropriate *m*/*z* range using multichannel analysis, and an external calibration was applied to the data to ensure mass accuracy.

## RESULTS

*Modification of the Nephrops 16-kDa Proteolipid by N-(1-Pyrenyl)cyclohexylcarbodiimide.* The *Nephrops* proteolipid was reactive toward PCD either in its native form (data not shown) or when expressed in *Saccharomyces* and integrated into the yeast V-ATPase (Figure 2A). Incubation of vacuolar membranes with PCD resulted in increased fluorescent yield which could be blocked by preincubation with DCCD. There was also an appreciable temperature effect, with an elevated rate of reaction at 30 °C (Figure 2A), likely to result from enhanced partitioning of the probe into the membrane. PCD was essentially nonfluorescent in the unreacted form (Figure 2A). Analysis by mass spectrometry (data not shown) indicated that >90% of the native proteolipid was modified after 3 h of incubation with PCD at 30 °C. The mass of the modified proteolipid was 16517.8 Da (±0.01%), corresponding to the proteolipid (16193.7 Da ± 0.01%) with a single PCD adduct of 324.1 Da. As the *Nephrops* proteolipid has been shown to be modified by [$^{14}$C]DCCD only at Glu140 (*27*), we conclude that the single PCD modification is also at this same residue.

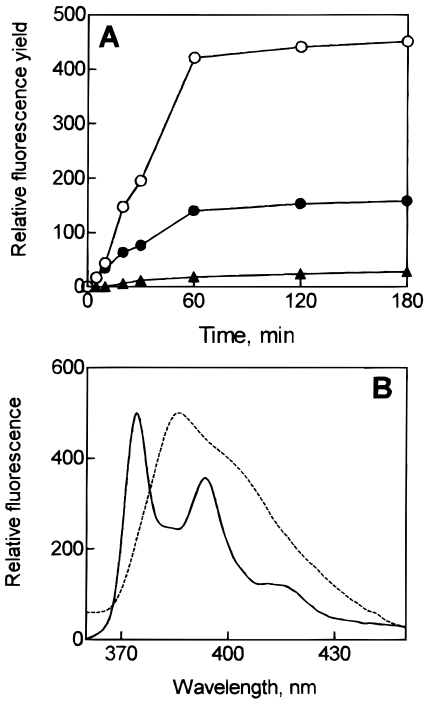


FIGURE 2: PCD modification of recombinant *Nephrops* 16-kDa proteolipid. (A) PCD labeling of vacuolar membranes from *Saccharomyces* expressing the *Nephrops* 16-kDa proteolipid. Membranes were incubated with the probe at 30 °C (open circles), at 30 °C after preincubation for 30 min with DCCD (triangles), or at room temperature (closed circles). Aliquots were removed at the specified time points, and the fluorescence yield at 375 nm was measured. (B) Fluorescence emission spectra of PCD-modified 16-kDa proteolipids. Spectra were recorded for vacuolar membranes containing recombinant *Nephrops* proteolipid (solid line) and for affinity-purified $V_0$ sectors containing the *Nephrops* proteolipid (hatched line). The excitation wavelength was 342 nm.

Fluorescence emission spectra of PCD-modified proteolipids (Figure 2B) were similar to those previously reported for pyrenyl species (for example, ref *28*). However, some qualitative differences in emission spectra were observed between detergent-solubilized forms of proteolipid, which exhibited a single emission maximum at 386 nm, and membrane-incorporated forms of labeled protein, which showed maxima at 376 and 395 nm. The spectral properties of the PCD adduct are likely therefore to be dependent on the local environment of the fluorophore. ATP-hydrolyzing activity was inhibited by both PCD and DCCD, with $I_{50}$ values approximately 40 and 20 $\mu$M, respectively, concomitant with complete inhibition of proton translocation (data not shown). Inhibition of proton translocation by DCCD has previously been widely reported (for example, refs *7* and *10*).

| | | | | | | | | | | | | | | | | | | | | | | | | | |
|---|---|---|---|---|---|---|---|---|---|---|---|---|---|---|---|---|---|---|---|---|---|---|---|---|---|
| | | | | | | | | | | | | | * | | | | | | | | | | | | |
| *E. coli* subunit c Helix 1 | 13 | A | A | V | M | M | G | L | A | A | I | G | A | A | I | G | I | G | I | L | G | 32 |
| *Nephrops* 16-kDa Helix 1 | 18 | A | A | S | A | M | V | F | S | A | L | G | A | A | Y | G | T | A | K | S | G | 37 |
| *Nephrops* 16-kDa Helix 3 | 96 | A | G | L | S | V | G | **L** | S | G | **L** | **A** | **A** | G | **F** | A | I | G | I | V | G | 115 |
| | | | | | | | | | | | | | * | | | | | | | | | | | | |
| *E. coli* subunit c Helix 2 | 54 | F | I | V | M | G | L | V | D | A | I | P | M | I | A | V | G | L | G | L | Y | 73 |
| *Nephrops* 16-kDa Helix 2 | 55 | I | I | P | V | V | **M** | **A** | **G** | I | **I** | A | I | **Y** | **G** | L | V | V | A | V | L | 74 |
| *Nephrops* 16-kDa Helix 4 | 133 | **I** | L | I | L | I | F | A | E | V | L | G | L | Y | G | **L** | I | V | A | I | F | 152 |

FIGURE 3: Sequence alignments of subunit c and the *Nephrops* 16-kDa proteolipid. N- and C-terminal halves of the 16-kDa proteolipid were aligned against the sequence of the *E. coli* subunit c using the program CLUSTAL. The positions of Asp61 and the complementary site Ala24, in helix 2 and helix 1 of subunit c, respectively, are indicated by asterisks. The sites within the *Nephrops* proteolipid mutated to glutamate are shown in bold and underlined. Numbers represent the positions of the first and last residues in each aligned segment.

*Glutamate Replacement Mutagenesis of the Nephrops Proteolipid*. The PCD labeling strategy was extended to a number of additional sites on the proteolipid, using mutagenically introduced glutamate residues as targets for modification. After expression in *Saccharomyces*, the extent to which each mutant proteolipid could be modified by PCD was used to assess exposure of the sites to the lipid phase. Individual glutamate residues were introduced into helices 2 and 3 of the E140G glutamate-less mutant *Nephrops* proteolipid. Sites were selected for glutamate reintroduction specifically to test the premise that the 16-kDa proteolipid represents a tandem repeat of the F-ATPase 8-kDa subunit c (*9*) and that it adopts a hexameric structure which parallels the dodecameric subunit c assembly (Figure 1). The preliminary model of the 16-kDa proteolipid, depicted in Figure 1, shows the predicted positions of key residues which are equivalent to residues with well-defined locations on the subunit c oligomer. Specifically, sequence alignments (Figure 3) indicate that Gly62 and Glu140 (in helices 2 and 4 of the 16-kDa proteolipid, respectively) represent equivalent positions in the first and second halves of the tandem repeat (*11*) and correspond to the position of the DCCD-reactive Asp61 of subunit c. Mutation of Asp61 to glycine in the *Escherichia coli* subunit c is lethal but can be suppressed by introduction of aspartate in place of Ala24 in the first helix of subunit c (*29*). The corresponding positions in the two tandem repeat elements constituting the 16-kDa proteolipid would be Ala29 in helix 1 and Ala107 in helix 3 (Figure 3). In this study we therefore introduced glutamates at, or close to, Ala107 and Gly62 in order to assess the exposure of these sites to the lipid phase (identified in Figure 3).

For the labeling strategy to be valid, it is essential that each mutant polypeptide adopt a fold which is not significantly different from that of the wild-type species. The criteria we have used for correct folding of the mutant proteolipids are targetting to the vacuolar membrane and integration into an assembled V-ATPase (*30*). The association of soluble $V_1$ subunits with the vacuolar membrane is absolutely dependent on the stable assembly of $V_0$, which in turn requires correct folding and assembly of the 16-kDa proteolipid (*30*). Migration of assembled V-ATPase complexes through glycerol gradients after detergent solubilization therefore provides an assay for correct folding and assembly of the mutant proteolipids. Enzyme complexes containing either wild-type or mutant *Nephrops* proteolipids showed very similar migration on glycerol gradients (Figure 4), with the peak of ATPase activity in the gradients comigrating with the $V_1$ subunit Vma2p and $V_0$ subunit

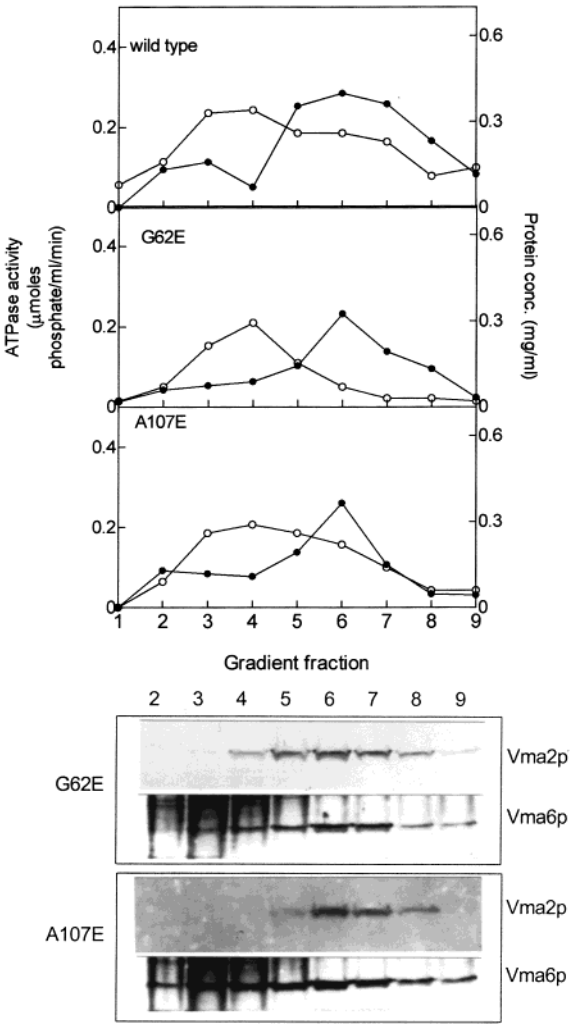


FIGURE 4: Assembly of hybrid V-ATPases containing the *Nephrops* 16-kDa proteolipid. Vacuolar membranes containing wild-type or glutamate replacement mutant forms of proteolipid were solubilized with 3% w/v dodecyl maltoside and fractionated by centrifugation on 20−50% glycerol gradients. Gradients were divided into nine equal fractions (fraction 1 is the uppermost fraction with lowest glycerol concentration) and assayed for protein concentration (open circles) and ATP hydrolyzing activity in the presence of sodium azide (0.05% w/v) (closed circles). Profiles for separations of membranes containing mutant proteolipids (examples shown are G62E and A107E) were essentially identical to those obtained with wild-type membranes (upper panel). Analysis of fractions by immunoblotting with antisera to $V_1$ (Vma2p) or $V_0$ subunits (Vma6p) showed comigration of both domains of the enzyme with ATPase activity to fractions containing approximately 40% glycerol (lower panel), diagnostic for assembly of high molecular mass mutant V-ATPases.

Table 1: Expression of Glutamate Replacement 16-kDa Proteolipids and Assembly of the V-ATPase: ATP-Hydrolyzing Activities of Vacuolar Membranes[a]

| | control rate | +NEM (%) | +DCCD (%) |
|---|---|---|---|
| wild type | 12.8 | 2.7 (21) | 3.2 (25) |
| E140G | 6.9 | 2.3 (33) | 6.8 (98) |
| I64E | 3.9 | 0.8 (20) | 4.0 (103) |
| L105E | 4.0 | 1.9 (48) | 4.0 (100) |
| A106E | 10.4 | 2.5 (24) | 10.0 (96) |
| A107E | 9.6 | 2.6 (27) | 9.8 (102) |

[a] Vacuolar membranes were isolated from *Saccharomyces* cells expressing glutamate replacement mutant 16-kDa proteolipids, and ATP hydrolyzing activities were determined from the rate of release of inorganic phosphate. Effects of inhibitor binding at either the $V_1$ or $V_0$ sectors of the V-ATPase were analyzed by incubation with NEM (50 $\mu$M for 30 min) or DCCD (100 $\mu$M for 1 h), respectively. Rates are expressed as $\mu$mol of phosphate (mg of protein)$^{-1}$ h$^{-1}$.

Vma6p. It is clear therefore that mutation of the proteolipid did not compromise its folding and assembly and that the structure of the mutant polypeptides adequately reflects the native fold. V-ATPases containing glutamate replacement proteolipids were also able to support uncoupled ATP hydrolysis which was DCCD-insensitive but was inhibited by NEM (Table 1). NEM modifies a cysteine residue adjacent to the nucleotide binding site of the V-ATPase, and inhibition by this compound is diagnostic for $V_1$-dependent ATPase activity (*31*). Complete assembly of V-ATPases incorporating inactive membrane subunits has previously been described for the E140G mutant of the *Nephrops* proteolipid (*32*), for the related Vma11p and Vma16p proteolipids (*33*), and for a number of mutants of the $V_0$ subunit Vph1p (*34*). None of the glutamate replacements were able to suppress the inhibitory effect of the initial E140G mutation, as judged by the failure of the mutant cDNAs to complement the pH-sensitive *vma3* phenotype and restore growth on test plates buffered to pH 7.5. Constitutive expression of the mutant proteolipids resulted in equivalent levels of 16-kDa proteolipid across all mutants studied (data not shown).

*Fluorometric Analysis of PCD Labeling.* The relative reactivity of the mutant proteolipids toward PCD was determined from the maximal fluorescence yield attained after incubation of vacuolar membranes with the probe (Figure 5). Only the A107E and (to a lesser extent) I64E proteolipids were labeled to levels which were significantly higher than those of the E140G background (see legend to Figure 5). Analysis of fluorescence yield from PCD-modified proteolipids purified by extraction into chloroform/methanol gave a pattern of labeling qualitatively similar to that found for vacuolar membranes, with significant labeling only in the case of wild-type, A107E, and I64E proteolipids (data not shown). All proteolipid preparations showed some fluorescence which could be reduced by preincubation with DCCD. The background labeling observed across the whole range of mutant proteolipids could arise from PCD modification of additional proteolipid species Vma11p and Vma16p which are presumed to be present in the vacuolar membrane at relatively low levels.

The environments of the pyrene fluorophores attached to either the wild-type or A107E mutant proteolipids were further characterized by fluorescence quenching analysis. PCD-labeled $V_0$ sectors, affinity purified via C-terminal hexahistidine tags on the proteolipid, were reconstituted into liposomes, and the fluorescence yield was titrated against concentration of cationic (acrylamide), anionic (iodide), or amphipathic (TEMPO) quenchers (Figure 6). Fluorescence from both wild-type and A107E mutant proteolipids was efficiently quenched by the lipid-soluble quencher TEMPO (Figure 6) but not by aqueous phase quenchers. The depth of the fluorophore in the bilayer was calculated by the parallax method, using PCD-labeled $V_0$ sectors reconstituted with lipid mixtures containing different mole ratios of phosphatidylcholine, spin-labeled at either the C5 or C12 positions in the acyl chain. This direct introduction of quencher lipid at the reconstitution stage largely eliminates any problems arising from differences in membrane partitioning properties of fatty acid quenchers spin-labeled at different positions. Although both forms of SLPC were able to quench pyrene fluorescence (Figure 7), the quenching did show some positional dependence, with the 5-SLPC species

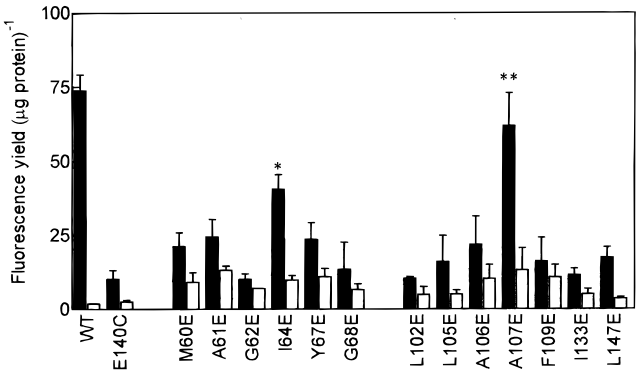


FIGURE 5: Differential PCD labeling of glutamate mutant proteolipids. The maximum fluorescence yield was recorded for vacuolar membranes from cells expressing each form of glutamate replacement proteolipid. Membranes were incubated either directly with PCD (filled bars) or with PCD after preincubation with 100 $\mu$M DCCD (open bars). Values are averages of at least four experiments. Analysis of variance (Dunnett's test) indicates that only the A107E ($p < 0.01$**) and I64E ($p < 0.05$*) mutant proteolipids are labeled to a level significantly higher than the E140G background mutant.

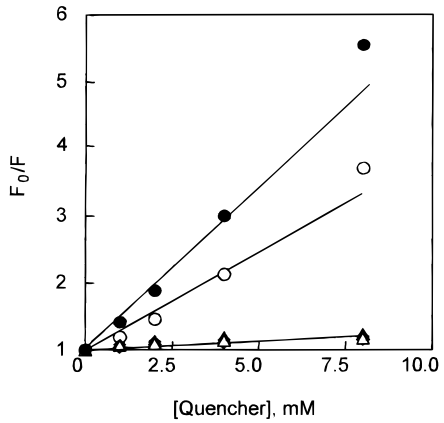


FIGURE 6: Differential effects of quenchers on PCD fluorescence. Affinity-purified, PCD-labeled $V_0$ sectors incorporating either wild-type (solid symbols) or A107E mutant (open symbols) proteolipids were reconstituted into liposomes, and the fluorescence yield at 375 nm was titrated against quencher concentration. Stern−Volmer plots of quenching by TEMPO (circles), acrylamide (triangles), or iodide (diamonds) indicate quenching only by the lipid-soluble species. $F$ and $F_0$ are the fluorescence yields in the presence and absence of quencher, respectively.

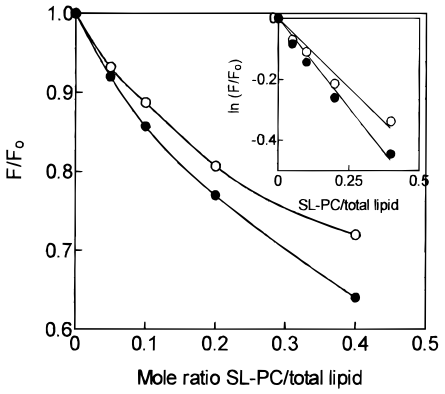


FIGURE 7: Quenching of fluorescence from PCD-labeled proteolipid reconstituted with spin-labeled lipids is dependent on both quencher concentration and depth of the spin-label. Affinity-purified $V_0$ sectors containing wild-type *Nephrops* proteolipid were reconstituted with lipid mixtures containing varying mole ratios of spin-labeled phosphatidylcholine substituted at the C5 (5-SLPC: closed circles) or C12 (12-SLPC: open circles) positions of the stearoyl chain, and the fluorescence yield from the pyrene adduct was measured. Typical data sets were used to calculate the depth of the fluorophore in the bilayer by the parallax method.

more effective. Calculations of distances between the fluorophore and bilayer center using data exemplified in Figure 7 gave values of $9 \pm 2$ and $9 \pm 4$ Å for wild-type and A107E mutant proteolipids, respectively.

## DISCUSSION

PCD reacts specifically with protonated carboxyls to form a stable, fluorescent *N*-acylurea end product only if water is excluded (*35*), making it particularly useful as a probe for carboxyl-containing residues at protein−lipid interfaces. The *Nephrops* 16-kDa proteolipid undergoes modification by this reagent with both high efficiency and specificity at a single site, Glu140, resulting in inhibition of ATPase activity and proton translocation. Modification of Glu140 indicates that the side chain of this key functional residue is at least partly accessible from the lipid phase of the bilayer. This inference is confirmed by fluorescence quenching studies, which show collisional interactions exclusively between the fluorophore and membrane-permeable quenchers. A distance of 9 Å between the fluorophore and bilayer center, calculated for both wild-type Glu140 and mutant Glu107 residues, would place the pyrene group attached to either site approximately midway through one leaflet of the membrane bilayer. Parallel studies using nonlinear ESR methods to measure interactions between spin-labeled fatty acids and Glu140 in native *Nephrops* membranes are in general agreement with the position of Glu140 in the V-ATPase membrane sector estimated from the studies described here (*13*). Maximum spin−spin interaction between the paramagnetic DCCD analogue *N*-(2,2,6,6-tetramethylpiperidineoxy)-*N*′-cyclohexylcarbodiimide attached to the proteolipid and stearic acid carrying the spin label at the C10 position also equates to a position for the modified Glu140 approximately 10 Å from the polar/hydrophobic boundary. The relative positions of charged or polar residues in the sequence of the 16-kDa proteolipid, which mark the approximate boundaries of the transmembrane helices (*11*), suggest that both sites would be within the cytoplasmic half of the membrane. The lipid exposure of Glu140, Ala107, and Ile64 and their relatively deep positions in the membrane have clear implications for both the mechanism of proton translocation by the V-ATPase and the organization of the proteolipid.

The data reported in this study provide independent experimental evidence in support of a model for the 16-kDa proteolipid hexamer (*18*). The fluorescent labeling and quenching data described in this study confirm not only that the functionally critical Glu140 is lipid-exposed but also that faces of helices 2 and 3 are in contact with the lipid phase. Indeed, it is the glutamate replacements at Ala107 and Ile64 which show quantitatively the highest degree of labeling, sites which according to the model would be predicted to be particularly accessible from the bilayer. The mutually supportive nature of the data obtained by two independent experimental approaches therefore goes some way to verifying the accuracy of the model. Current structural models of the subunit c oligomer, which accommodate available NMR, cross-linking, and mutagenesis data, indicate that Asp61 and Ala24 are at equivalent depths in the membrane. The finding that the equivalent sites in the 16-kDa proteolipid are also at similar depths in the bilayer is further support for the suggestion that the structure of the helix 3−helix 4 element of the 16-kDa proteolipid mirrors that of subunit c.

A number of hypothetical mechanisms which could couple ATP-driven rotation to proton movement have been proposed for both F-ATPase (*15*, *36*−*38*) and V-ATPase (*39*). Most of these models (but not all; see ref *40*) require that the intramembrane acidic residue must, at some stage in the enzyme cycle, be exposed to the lipid in a neutral, protonated state. A proton translocation pathway is proposed to form when rotation of the subunit c oligomer brings the protonated Asp61 into contact with a static $F_0$ component, subunit a (*15*, *36*−*38*). Although the relative movement of the two components has yet to be demonstrated experimentally, a quantitative assessment of the hypothetical mechanism has shown that it is consistent with the thermodynamic and mechanical properties of the F-ATPase (*41*). The data presented in this study show conclusively that the protonated Glu140 of the 16-kDa proteolipid is exposed to the hydrophobic core of the membrane, sited at the external surface of the $V_0$ sector. The proton pathway in $V_0$ may therefore be constituted in a way similar to that suggested for $F_0$, requiring a functional interaction between the 16-kDa proteolipid and another integral membrane subunit equivalent to subunit a. A mutagenic study of another $V_0$ subunit, the product of the *Saccharomyces VPH1* gene (Vph1p), has identified a number of residues which are involved in proton translocation (*42*), leading to the suggestion that this subunit may be a functional homologue of subunit a. According to our model, it would be the external, lipid-exposed surface formed at the helix 2−helix 4 junction which would constitute the key region of contact between proteolipid and Vph1p (see Figure 1).

Despite a number of differences in both the composition and functional properties of the F- and V-ATPases, we suggest that there may be some convergence with regard to the fundamental mechanisms of the two classes of enzyme. Although constructed from protein subunits with quite distinct structural differences, the proton pathways of $V_0$ and $F_0$ appear to share a number of properties. While it remains to be demonstrated, this then leads to the suggestion that

the basic engine of the V-ATPase may be, as for the $F_1$-ATPase, subunit rotation driven by ATP hydrolysis.

## ACKNOWLEDGMENT

We are grateful to Prof. Nathan Nelson (Tel Aviv University) for making available the *vma3* yeast strain, to Prof. R. Serrano (Polytechnic University, Valencia) for providing a *PMA1* plasmid, and to Prof. Tom Stevens (University of Oregon) for providing antisera.

## REFERENCES

1. Finbow, M. E., and Harrison, M. A. (1997) *Biochem. J. 324*, 697−712.
2. Stevens, T. H., and Forgac, M. (1997) *Annu. Rev. Cell. Dev. Biol. 13*, 779−808.
3. Boekema, E. J., Ubbink-Kok, T., Lolkema, J. S., Brisson, A., and Konings, W. N. (1997) *Proc. Natl. Acad. Sci. U.S.A. 94*, 14291−14293.
4. Wilkens, S., and Capaldi, R. A. (1998) *Nature 393*, 29.
5. Noji, H., Yasuda, R., Yoshida, M., and Kinosita, K. (1997) *Nature 386*, 299−302.
6. Sambongi, Y., Iko, Y., Tanabe, M., Omote, H., Iwamoto-Kihara, A., Ueda, I., Yanagida, T., Wada, Y., and Futai, M. (1999) *Science 286*, 1722−1724.
7. Arai, H., Berne, M., and Forgac, M. (1987) *J. Biol. Chem. 262*, 11006−11011.
8. Fillingame, R. H. (1996) *Curr. Opin. Struct. Biol. 6*, 491−498.
9. Mandel, M., Moriyama, Y., Hulmes, J. D., Pan, Y. E., Nelson, H., and Nelson, N. (1988) *Proc. Natl. Acad. Sci. U.S.A. 85*, 5521−5524.
10. Harrison, M. A., Jones, P. C., Kim, Y. I., Finbow, M. E., and Findlay, J. B. C. (1994) *Eur. J. Biochem. 221*, 111−120.
11. Holzenburg, A., Jones, P. C., Franklin, T., Pali, T., Heimburg, T., Marsh, D., Findlay, J. B. C., and Finbow, M. E. (1993) *Eur. J. Biochem. 13*, 21−30.
12. John, S. A., Saner, D., Pitts, J. D., Holzenburg, A., Finbow, M. E., and Lal, R. (1997) *J. Struct. Biol. 120*, 22−31.
13. Páli, T., Finbow, M. E., and Marsh, D. (1999) *Biochemistry 38*, 14311−14319.
14. Girvin, M. E., Rastogi, V. K., Abildgaard, F., Markley, J. L., and Fillingame, R. H. (1998) *Biochemistry 37*, 8817−8824.
15. Rastogi, A., and Girvin, M. E. (1999) *Nature 402*, 263−268.
16. Jones, P. C., Jiang, W. P., and Fillingame, R. H. (1998) *J. Biol. Chem. 273*, 17178−17185.
17. Fillingame, R. H., Jones, P. C., Jiang, W., Valiyaveetil, F. I., and Dmitriev, O. Y. (1998) *Biochim. Biophys. Acta 1365*, 135−142.
18. Harrison, M. A., Murray, J., Powell, B., Kim, Y.-I., Finbow, M. E., and Findlay, J. B. C. (1999) *J. Biol. Chem. 274*, 25461−25470.
19. Jones, P. C., Harrison, M. A., Kim, Y. I., Finbow, M. E., and Findlay, J. B. C. (1995) *Biochem. J. 312*, 739−747.
20. Pringle, J. M., and Taber, M. (1985) *Biochemistry 24*, 7366−7371.
21. Landt, O., Grunert, H., and Hahn, U. (1990) *Gene 96*, 125−128.
22. Ito, H., Fukuda, Y., Murata, K., and Kimura, A. (1983) *J. Bacteriol. 153*, 163−168.
23. Uchida, E., Ohsumi, Y., and Anraku, Y. (1985) *J. Biol. Chem. 260*, 1090−1095.
24. Knol, J., Veehoff, L., Liang, W.-J., Henderson, P. J. F., and Poolman, B. (1996) *J. Biol. Chem. 271*, 15358−15366.
25. Chattopadhyay, A., and London, E. L. (1987) *Biochemistry 26*, 39−45.
26. Cruz, A., Casals, C., Plasencia, I., Marsh, D., and Perez-Gil, J. (1998) *Biochemistry 37*, 9488−9496.
27. Finbow, M. E., Eliopoulos, E. E., Jackson, P. J., Keen, J. N., Meagher, L., Thompson, P., Jones, P. C., and Findlay, J. B. C. (1992) *Protein Eng. 5*, 7−15.
28. Narayanaswami, V., Kim, J., and McNamee, M. G. (1993) *Biochemistry 32*, 12413−12419.
29. Miller, M. J., Oldenburg, M., and Fillingame, R. H. (1990) *Proc. Natl. Acad. Sci. U.S.A. 87*, 4900−4904.
30. Kane, P. M., Kuehn, M. C., Howald-Stevenson, I., and Stevens, T. H. (1992) *J. Biol. Chem. 267*, 447−454.
31. Moriyama, Y., and Nelson, N. (1987) *J. Biol. Chem. 262*, 14723−14729.
32. Hughes, G., Harrison, M. A., Kim, Y.-I., Griffiths, D. E., Finbow, M. E., and Findlay, J. B. C. (1996) *Biochem. J. 317*, 425−431.
33. Hirata, R., Graham, L. A., Takatsuki, A., Stevens, T. H., and Anraku, Y. (1997) *J. Biol. Chem. 272*, 4795−4803.
34. Leng, X. H., Manolson, M. F., Liu, Q., and Forgac, M. (1996) *J. Biol. Chem. 271*, 22487−22493.
35. Hassinen, I. E., and Vuokila, P. T. (1993) *Biochim. Biophys. Acta 1143*, 107−124.
36. Fillingame, R. H. (1997) *J. Exp. Biol. 200*, 217−224.
37. Junge, W., Lill, H., and Engelbrecht, S. (1997) *Trends Biochem. Sci. 22*, 420−423.
38. Vik, S. B., and Antonio, B. J. (1994) *J. Biol. Chem. 269*, 30364−30369.
39. Harrison, M. A., Finbow, M. E., and Findlay, J. B. C. (1997) *Mol. Membr. Biol. 14*, 1−3.
40. Kaim, G., and Dimroth, P. (1998) *EMBO J. 17*, 5887−5895.
41. Elston, T., Wang, H., and Oster, G. (1998) *Nature 391*, 510−513.
42. Zhang, J., Feng, Y., and Forgac, M. (1994) *J. Biol. Chem. 269*, 23518−23523.

BI000159O